



**HAL**  
open science

## **New membranes based on polyethersulfone – SlipSkin™ polymer blends with low fouling and high blood compatibility**

Odyl ter Beek, Denys Pavlenko, M. Suck, S. Helfrich, Lydia A.M Bolhuis-Versteeg, Dmytro Snisarenko, Christel Causserand, Patrice Bacchin, Pierre Aimar, René van Oerle, et al.

### **► To cite this version:**

Odyl ter Beek, Denys Pavlenko, M. Suck, S. Helfrich, Lydia A.M Bolhuis-Versteeg, et al.. New membranes based on polyethersulfone – SlipSkin™ polymer blends with low fouling and high blood compatibility. *Separation and Purification Technology*, 2019, 225, pp.60-73. 10.1016/j.seppur.2019.05.049 . hal-02291068

**HAL Id: hal-02291068**

**<https://hal.science/hal-02291068>**

Submitted on 18 Sep 2019

**HAL** is a multi-disciplinary open access archive for the deposit and dissemination of scientific research documents, whether they are published or not. The documents may come from teaching and research institutions in France or abroad, or from public or private research centers.

L'archive ouverte pluridisciplinaire **HAL**, est destinée au dépôt et à la diffusion de documents scientifiques de niveau recherche, publiés ou non, émanant des établissements d'enseignement et de recherche français ou étrangers, des laboratoires publics ou privés.






## Open Archive Toulouse Archive Ouverte (OATAO)

OATAO is an open access repository that collects the work of Toulouse researchers and makes it freely available over the web where possible

This is an author's version published in: <http://oatao.univ-toulouse.fr/24228>

**Official URL:** <https://doi.org/10.1016/j.seppur.2019.05.049>

### **To cite this version:**

Ter Beek, Odyl and Pavlenko, Denys and Suck, M. and Helfrich, S. and Bolhuis-Versteeg, Lydia A.M and Snisarenko, Dmytro  and Causserand, Christel  and Bacchin, Patrice  and Aimar, Pierre and van Oerle, René and Wetzels, Rick J.H. and Verhezen, Paul and Henskens, Yvonne and Stamatialis, Dimitrios *New membranes based on polyethersulfone – SlipSkin™ polymer blends with low fouling and high blood compatibility.* (2019) *Separation and Purification Technology*, 225. 60-73. ISSN 1383-5866

Any correspondence concerning this service should be sent to the repository administrator: [tech-oatao@listes-diff.inp-toulouse.fr](mailto:tech-oatao@listes-diff.inp-toulouse.fr)

# New membranes based on polyethersulfone – SlipSkin™ polymer blends with low fouling and high blood compatibility

O. ter Beek<sup>a</sup>, D. Pavlenko<sup>b</sup>, M. Suck<sup>a</sup>, S. Helfrich<sup>a</sup>, L. Bolhuis-Versteeg<sup>a</sup>, D. Snisarenko<sup>c</sup>, C. Causserand<sup>c</sup>, P. Bacchin<sup>c</sup>, P. Aimar<sup>c</sup>, R. van Oerle<sup>d</sup>, R. Wetzels<sup>e</sup>, P. Verhezen<sup>e</sup>, Y. Henskens<sup>e</sup>, D. Stamatialis<sup>a,\*</sup>

<sup>a</sup> (Bio)Artificial Organs, Department of Biomaterials Science and Technology, TechMed Centre, Faculty of Science and Technology, University of Twente, Drienerlolaan 5, 7500 AE Enschede, the Netherlands

<sup>b</sup> European Membrane Institute (EMI) Twente, University of Twente, Drienerlolaan 5, 7500 AE Enschede, the Netherlands

<sup>c</sup> Laboratoire de Génie Chimique, Université de Toulouse, CNRS, INPT, UPS, Université Toulouse III - Paul Sabatier, 118 route de Narbonne 31062, Toulouse CEDEX 9, France

<sup>d</sup> Laboratory for Clinical Thrombosis and Hemostasis, Maastricht University Medical Center, Universiteitssingel 50, 6200 MD Maastricht, the Netherlands

<sup>e</sup> Central Diagnostic Laboratory, Unit for Hemostasis and Transfusion, Maastricht University Medical Center, P. Debyelaan 25, 6229 HX Maastricht, the Netherlands

## ARTICLE INFO

**Keywords:**  
Hemodialysis  
Membrane  
Fouling  
Biocompatibility

## ABSTRACT

Hemodialysis is an important therapy for treating patients with End Stage Renal Disease (ESRD). These patients visit the hospital 3 times a week and each time their blood is cleansed during 4-hour dialysis sessions using a hollow fiber membrane module; also called artificial kidney. This device mainly achieves removal of small water-soluble toxins and a limited number of middle molecules. To improve the clearance of toxins, especially middle molecules and protein bound toxins, longer treatment via nocturnal dialysis and/or the application of portable/wearable artificial kidney is required. Such therapies require application of membranes with very low fouling and very good blood compatibility. Current membranes often contain hydrophilic additives which could elute during sterilization processes and/or during long-term filtration. In this study, we propose a simple method for developing low fouling blood compatible membranes by blending of polyethersulfone (PES), a material already used for fabrication of dialysis membranes, with small amounts of SlipSkin™ (SS), a blood compatible random copolymer of hydrophilic N-vinylpyrrolidone (NVP) and hydrophobic N-butylmethacrylate (BMA). Our results show that membranes with 2 wt% of SS have high fouling resistance to proteins and middle-size molecules and very good blood compatibility, making these membranes promising for application in dialysis therapy.

## 1. Introduction

Hemodialysis is an important therapy for End Stage Renal Disease (ESRD) patients if a donor kidney is not available. During four hours of conventional therapy, small water-soluble toxins with molecular weights (MW) lower than 500 Da and a limited number of middle molecules with MW in the range of 500–32,000 Da are effectively removed from the patients' blood [1–3]. However, more time is needed to improve the clearance of, for example, middle molecules such as  $\beta_2$ -microglobulin, because these toxins are mainly present in the intracellular space [4]. Therefore, many developments in hemodialysis

focus on longer treatment times, such as, nocturnal dialysis or even the application of a portable or wearable artificial kidney [4–8]. For these types of therapies, the contact time between the patients' blood and the dialyzer is prolonged and therefore, long-term membrane selectivity, fouling resistance and blood compatibility are generally required [2].

Current hemodialysis membranes are often based on blends of hydrophobic polymers, such as, polysulfone (PSu) or polyethersulfone (PES), with hydrophilic additives, such as, polyvinylpyrrolidone (PVP) or polyethylene glycol (PEG) [9]. The creation of hydrophilic and hydrophobic patches, especially on the membrane surface in contact with blood, decreases the protein adsorption there and therefore increases

\* Corresponding author at: (Bio)Artificial Organs, Department of Biomaterials Science and Technology, TechMed Centre, Faculty of Science and Technology, University of Twente, PO Box 217, Drienerlolaan 5, 7500 AE Enschede, the Netherlands.

E-mail addresses: [o.e.m.terbeek@utwente.nl](mailto:o.e.m.terbeek@utwente.nl) (O. ter Beek), [d.pavlenko@utwente.nl](mailto:d.pavlenko@utwente.nl) (D. Pavlenko), [m.h.suck@student.utwente.nl](mailto:m.h.suck@student.utwente.nl) (M. Suck), [l.a.m.bolhuis-versteeg@utwente.nl](mailto:l.a.m.bolhuis-versteeg@utwente.nl) (L. Bolhuis-Versteeg), [caussera@chimie.ups-tlse.fr](mailto:caussera@chimie.ups-tlse.fr) (C. Causserand), [bacchin@chimie.ups-tlse.fr](mailto:bacchin@chimie.ups-tlse.fr) (P. Bacchin), [aimar@chimie.ups-tlse.fr](mailto:aimar@chimie.ups-tlse.fr) (P. Aimar), [rene.vanoerle@maastrichtuniversity.nl](mailto:rene.vanoerle@maastrichtuniversity.nl) (R. van Oerle), [rick.wetzels@mumc.nl](mailto:rick.wetzels@mumc.nl) (R. Wetzels), [paul.verhezen@mumc.nl](mailto:paul.verhezen@mumc.nl) (P. Verhezen), [yvonne.henskens@mumc.nl](mailto:yvonne.henskens@mumc.nl) (Y. Henskens), [d.stamatialis@utwente.nl](mailto:d.stamatialis@utwente.nl) (D. Stamatialis).

<https://doi.org/10.1016/j.seppur.2019.05.049>

the membranes' fouling resistance and blood compatibility [10–13]. However, the hydrophilic additives, such as PVP, can elute from the membrane matrix due to wall shear stress during ultrafiltration or as the result of some sterilization techniques [14–17]. For example, membrane sterilization via autoclaving results in less cross-linked PVP than sterilization via gamma-radiation, which could result in elution of PVP during long-term dialysis therapy [18]. As a consequence, the membrane's structural characteristics and filtration performance would be compromised [14,15,18,19]. Besides, the eluted PVP can be potentially harmful to patients because it can accumulate in internal organs and induce allergies and anaphylactic shock [19–21].

Alternative methods to improve membrane compatibility and fouling resistance include coating or grafting of hydrophilic polymers onto membranes' surfaces. For example, coating a PES membrane with graphene oxide and sulfonated polyanion hydrogel thin film can enhance the membrane hydrophilicity [20,22,23]. However, the coating there is not covalently bound and during dialysis sessions it can be detached from the membrane due to the blood flow and the associated shear stress [14,20,22]. Grafting of hydrophilic polymers onto membranes' surfaces, for example, heparin-mimicking polymer brushes onto functionalized carbon nanotube/ PES composite membranes has also been reported [24]. This method is more stable and can significantly improve the anti-fouling performance of membranes. However, it requires a rather elaborate chemistry which cannot be easily implemented during the fabrication process of hollow fiber membranes [24].

In this work, we investigate a simple method for preparing low fouling blood compatible membranes for dialysis by blending PES with SlipSkin™ (50:50) (indicated as PES-SS). The SlipSkin™ (50:50) (SS) is a random copolymer of 50:50 ratio of hydrophilic N-vinylpyrrolidone (NVP) and hydrophobic N-butylmethacrylate (BMA) originally developed for coating of catheters and guide wires for intravascular interventions (Fig. 1) [25–27]. The advantage of using SS for membrane preparation is that both hydrophilic and hydrophobic blocks contribute to the membranes' blood compatibility and fouling resistance [2,28]. In earlier work, we developed pristine SS membranes based on various ratio of NVP and BMA. The membranes with 50:50 ratio showed excellent blood compatibility, but they had high water permeance, of 100–200 L m<sup>-2</sup> h<sup>-1</sup> bar<sup>-1</sup> but also very high albumin leakage (BSA sieving coefficient (SC) was 0.83). This is undesirable, since the typical membranes for dialysis therapy should have little or no albumin leakage (SC for albumin should be around 0.015) [29]. Besides, due to the rather high amounts of the hydrophilic component NVP, these SS membranes swell significantly in aqueous solutions and require delicate handling for achieving stable filtration performance using these solutions. Here, we investigate whether membranes based on PES-SS polymer blends with low amounts of SS (2–6 wt%) would combine the positive characteristics of SS (high hydrophilicity, low fouling, good blood compatibility) with the positive characteristics of PES (good membrane formation, minimal swelling).

We first produce flat-sheet PES-SS membranes, the morphology and chemistry of which are thoroughly characterized via Scanning Electron Microscopy (SEM) and Attenuated Total Reflectance-Fourier Transform Infrared spectroscopy (ATR-FTIR), respectively. Their fouling resistance

is investigated using model protein solutions of BSA (MW = 66 kDa), which should be retained by the membrane, and of  $\alpha$ -Lactalbumin (LALBA, MW = 14 kDa), as representative of middle size molecules which should be removed during the dialysis treatment. Finally, we also perform extensive blood compatibility studies of the optimal membranes, following the ISO guideline 10993: 'Biological evaluation of medical devices, part 4, selection of tests for interactions with blood' [30]. These blood compatibility tests include platelet adhesion and aggregation tests (thrombosis category), classical and alternative pathway complement activity tests (complement category), thrombin generation tests (coagulation category), and adhesion of leukocytes and hemolysis tests (hematology category). The results are compared to custom-made PES and PES-PVP membranes as well as to commercially available PES membranes.

## 2. Materials and methods

### 2.1. Materials

SlipSkin™ (50:50) (SS), a copolymer of N-vinylpyrrolidone (NVP) and N-butylmethacrylate (BMA) (kindly provided by Interface BIOMaterials BV, Geleen, The Netherlands), polyethersulfone (PES) (ULTRASON, E6020P, BASF, Arnhem, The Netherlands) and polyvinylpyrrolidone (PVP) (K90, MW  $\approx$  360 000) (Fluka, Sigma-Aldrich, Germany) were used to prepare the membranes. N-methyl-2-pyrrolidone (NMP) (Acros Organics, Geel, Belgium) was used as solvent. PES membranes (molecular weight cut-off, MWCO of 50 kDa), purchased from Sartorius, Göttingen, Germany, indicated PES-50 kDa) were used as reference. A Milli-Q purification unit (Merck Millipore, Czech Republic) was used to prepare ultrapure water. Ultrapure water was used as a non-solvent in the coagulation bath and for transport experiments. Phosphate-buffered saline (PBS) (pH 7.45, GibCo, United Kingdom), bovine serum albumin (BSA) and  $\alpha$ -Lactalbumin (LALBA) from bovine milk both purchased from Sigma-Aldrich (Zwijndrecht, The Netherlands) were used to evaluate membranes' transport properties and fouling resistance. An Atto 647 N Protein Labeling Kit was purchased from Sigma-Aldrich (France) for the microchip fouling experiments on the PES-50 kDa and custom-made PES-SS membranes. Glass coverslips (VWR, Amsterdam, The Netherlands) were used as positive control. All chemicals necessary for the blood compatibility tests, such as the thrombin generation tests, lactate dehydrogenase assays, hematology and complement tests, were the same as stated in previous work [2].

### 2.2. Membrane preparation

Flat-sheet membranes were prepared by casting polymer solutions dissolved in NMP. To obtain homogeneous polymer solutions, we blended PES and small amounts of SS (2–6 wt%). As references, custom-made flat-sheet membranes from 15 wt% PES dissolved in NMP, custom-made flat-sheet membranes from 15 wt% PES and 7 wt% PVP dissolved in NMP and PES-50 kDa membranes from Sartorius were used. Membranes based on SS alone were also prepared for ATR-FTIR studies. For this, 15 wt% SS was dissolved in NMP. All membranes used

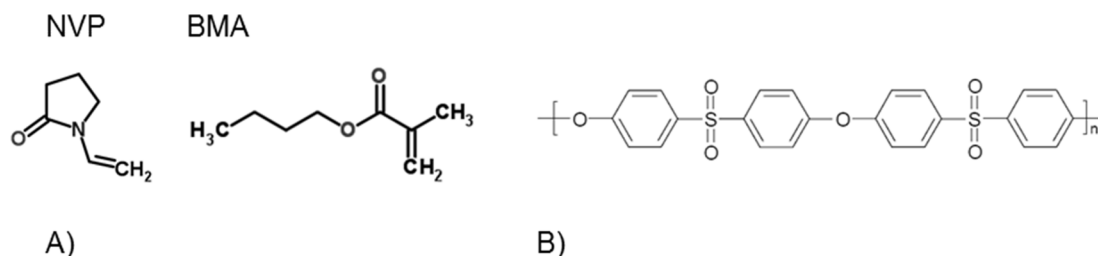


Fig. 1. Chemical structures of (A) SlipSkin™ copolymer with N-vinylpyrrolidone (NVP) and n-butylmethacrylate (BMA) and (B) polyethersulfone (PES).

**Table 1**

Codes and details of membranes used in this study.

Code	Polymer (ratio in polymer solution)	Additive (ratio in polymer solution)	Solvent	Manufacturer
PES-PVP	PES 15 wt%	PVP 7 wt%	NMP	this work
PES-SS2	PES 15 wt%	SlipSkin™ 2 wt%	NMP	this work
PES-SS4	PES 15 wt%	SlipSkin™ 4 wt%	NMP	this work
PES-SS6	PES 15 wt%	SlipSkin™ 6 wt%	NMP	this work
PES	PES 15 wt%	–	NMP	this work
PES-50 kDa	PES	–	–	Sartorius
SS	SlipSkin™ 15 wt%	–	NMP	this work
RC58	regenerated cellulose	–	–	Whatman, Sigma-Aldrich
DE81	DEAE cellulose	–	–	Whatman, Sigma-Aldrich

are listed in [Table 1](#). The number in the codes of the PES-SS blend membranes refers to the weight percentage of SS used in the polymer solution. The polymer solutions were mixed on a roller bank at room temperature and degassed overnight before membrane preparation. All membranes were prepared by phase inversion. The polymer solutions were cast on a glass plate using a casting knife of 300  $\mu\text{m}$  thickness, and afterwards immediately immersed in a non-solvent ultrapure water coagulation bath. The membranes were rinsed thoroughly and stored in ultrapure water for subsequent characterization.

Regenerated cellulose RC58 (Whatman, Sigma-Aldrich) and DEAE cellulose DE81 (Whatman, Sigma-Aldrich) commercial membranes were used, as controls, in the blood compatibility studies.

### 2.3. Membrane characterization

#### 2.3.1. Scanning electron microscopy (SEM)

The membranes were dried overnight in air and broken cryogenically in liquid nitrogen to obtain cross-sections. The samples were placed in SEM holders and gold coated using a Cressington 108 auto-sputter coater. Then, the membranes ( $n = 3$ ) were characterized using a Jeol JSM-IT 100 LV scanning electron microscope and InTouchScope™ software.

#### 2.3.2. Attenuated total reflectance-Fourier transform infrared spectroscopy (ATR-FTIR)

Analysis of the membrane surface was performed on dried samples by ATR-FTIR spectroscopy (Spectrum Two, PerkinElmer) and Spectrum Quant software. All scans were performed in triplicate on various parts of the membrane surface ( $n = 3$ ), at a resolution of  $4\text{ cm}^{-1}$  and at room temperature.

#### 2.3.3. Membrane transport properties

To determine the membranes' transport properties, an air-pressurized dead-end Amicon ultrafiltration cell (3 mL, Amicon®- Merck Millipore) with a  $0.9\text{ cm}^2$  effective membrane area was used. The selective layer of the membrane was exposed to the (protein) solutions. First, the membranes were pre-compacted with ultrapure water at a transmembrane pressure (TMP) of 1500 mmHg for 30 min. Then, the amount of permeated water was measured over time at TMPs of 375, 750, 1125 and 1500 mmHg. The ultrafiltration (UF) coefficient ( $\text{L m}^{-2}\text{ h}^{-1}\text{ mmHg}^{-1}$ ) was calculated as the slope of the linear fit of the flux ( $\text{L m}^{-2}\text{ h}^{-1}$ ) versus TMP graph. After this, the sieving and anti-fouling properties of the membranes were determined. First, the membranes were wetted and pre-compacted using ultrapure water at transmembrane pressure (TMP) of 1 bar for 30 min. After this, ultrapure water was pressurized through the membranes at 1 bar for 1 h and the flux,  $J$  ( $\text{L m}^{-2}\text{ h}^{-1}$ ), of the water through the membranes was determined by taking the permeated water volume, membrane surface area and time at each pressure into account. Then, the ultrapure water was replaced

rapidly by a protein solution – either a BSA solution of 1 mg/mL or a LALBA solution of 1 mg/mL – and the solution was stirred at a 300-rpm stirring rate. A pressure of 1 bar was applied for 1 h and the permeate was collected in order to calculate the protein solutions' flux. After the experiment with proteins, the Amicon cell was filled with ultrapure water again and the membranes were washed for 30 min. Finally, the clean water flux of the membranes after protein solution transport was investigated using ultrapure water and a pressure of 1 bar for 1 h. The fouling resistance of the membranes was assessed in triplicate via the flux recovery ratio:

$$\text{flux recovery ratio (FRR)} = \frac{J_{w,2}}{J_{w,1}} \cdot 100\% \quad (1)$$

where  $J_{w,1}$  is the first clean water flux measurement ( $\text{L m}^{-2}\text{ h}^{-1}$ ) and  $J_{w,2}$  is the clean water flux measurement ( $\text{L m}^{-2}\text{ h}^{-1}$ ) after the protein filtration experiment. The higher the FRR the higher the membrane fouling resistance.

To determine the protein sieving coefficient (SC) of the membranes ( $n = 3$ ), 2 mL samples of the permeate and retentate solutions were taken as soon as the protein solution transport measurements were completed. The BSA and LALBA concentrations were determined using a UV-spectrophotometer (Varian, Cary 300 Scan UV-visible spectrophotometer) at 280 nm. The SC was calculated as follows:

$$\text{SC} = \frac{C_{\text{permeate}}}{C_{\text{retentate}}} \quad (2)$$

where  $C_{\text{permeate}}$  is the concentration of BSA or LALBA (mg/mL) in the permeate solution and  $C_{\text{retentate}}$  is the BSA concentration or LALBA concentration (mg/mL) in the retentate solution. A SC of 1 means that the proteins pass freely through the membrane, while a SC of 0 means that all proteins are fully retained by the membrane.

#### 2.3.4. Microfluidic chip fouling experiments

To monitor the fouling of LALBA to the membranes over time at zero transmembrane pressure (TMP), we used a microchip. All membranes were measured in triplicate. LALBA was first labelled following the protocol proposed by Greene et al. [31]. More information about this protocol can be found in [Appendix A](#). The final conjugate solution was diluted with PBS to achieve a concentration of 50 mg/L, corresponding to clinically relevant median concentrations of  $\beta_2$ -microglobulin in human blood [3]. Then, the microfluidic chips were connected to a pressure-flow controller and placed on a microscope stage. More information about the experimental set-up can be found in [Appendix A](#) and [Fig. A1](#).

Before the fouling resistance experiment was started, the membranes were wetted for 1 h. For this, pure PBS was flowed through the microchip at 130  $\mu\text{L}/\text{min}$  (this flow rate corresponds to a Reynolds number of 4.7) and zero pressure was applied from the permeate side. Next, the labelled LALBA was flowed through the microchip at three different flow rates (35, 75 and 130  $\mu\text{L}/\text{min}$ ), all in a single pass, which means that the feed solution, after reaching the retentate reservoir, was not resupplied to the system. The control over the cross-flow velocity TMP was done by adjustments of the pressures at the inlet, the retentate, and the permeate reservoirs. Finally, the fluorescence on the membrane surface at the retentate compartment of the microchip was estimated: images of the whole channel were acquired every 5 min using a Cy5 filter. The gray value as a unit of fluorescence intensity was measured using ImageJ software. A high gray value corresponds to high fluorescence (more white pixels). To evaluate the effect of flow rate on membrane fouling, three feed flow rates of 35, 75, and 130  $\mu\text{L}/\text{min}$  were applied. Moreover, the spatial distribution of fouling along the membrane was evaluated using gray value analysis at three different positions in the channel: at the inlet, in the middle, and at the outlet. The gray value of each pixel along the line of the channel was measured, yielding an average gray value with its respective standard deviation.

### 2.3.5. Blood compatibility tests

We performed extensive blood compatibility studies of the membranes following the ISO guideline 10993: 'Biological evaluation of medical devices, part 4, selection of tests for interactions with blood'. We examined the following:

- Platelet adhesion and aggregation, for the thrombosis category
- Classical and alternative pathway complement activity, for the complement category
- Thrombin generation, for the coagulation category
- Adhesion of leukocytes and hemolysis, for the hematology category

The detailed protocols for the biocompatibility tests were published earlier [2]. Here, we present a few adjustments done. For the qualitative platelet adhesion tests, fresh blood from three healthy volunteers (donors, 4, 5 and 6; all donors gave informed consent) was taken in Vacuette precipitated tubes. The whole blood was anticoagulated with citrate (11 mM) and platelet rich plasma (PRP) was obtained by centrifugation. Then, 300  $\mu\text{L}$  of PRP was added to the membranes and glass coverslips (positive control) on the bottom of 24 well plates in duplo. The PRP was removed after 45 min incubation time at 37 °C and the samples were washed three times using PBS. Then, all samples were incubated with 900  $\mu\text{L}$  of 2.5% glutaraldehyde and after 1 h at 4 °C the samples were washed with 0.1 M phosphate buffer (pH = 7.2) and ultrapure water. Finally, the samples were dried and analysed using SEM. For the quantitative platelet adhesion tests using the lactate dehydrogenase (LDH) assay, 250  $\mu\text{L}$  PRP from donors 4, 5 and 6 was added to all samples on the bottom of 96 well plates for 60 min at 37 °C in duplo. After removal of the PRP, the samples were washed with PBS three times and incubated in 200  $\mu\text{L}$  lysis buffer for 60 min at room temperature. Then, 50  $\mu\text{L}$  of supernatant and 50  $\mu\text{L}$  substrate mix were added to the wells of a clean 96 well plate (in duplo). After 30 min incubation time in the dark, 50  $\mu\text{L}$  stop solution was added to all wells. Subsequently, the optical density was measured at 490 nm using a microplate reader and the platelets were quantified using a standard curve.

For the complement activation tests, fresh blood from donors 1, 2 and 3 (healthy volunteers, all donors gave informed consent) was collected in BD Vacutainer SSTII Advance tubes (BD Plymouth, UK). Then, 800  $\mu\text{L}$  of serum was used to incubate the samples on the bottom of 24 well plates (in duplo) for one hour at 37 °C under gentle shaking. The non-incubated serum control samples were frozen immediately. The activation of the classical and alternative pathway of the complement system were measured and analysed by ELISA using the WIESLAB® complement system kits for classical and alternative pathway (Euro Diagnostica, Sweden). For both the classical pathway and alternative pathway kit, the amount of C5b-9 complex formed on the plate surface was detected with a specific alkaline phosphatase labelled antibody to the C5b-9 neoantigen formed during membrane attack complex formation.

For the thrombin generation test, triplicates of membrane pieces and glass cover slips were put on the bottom of 24 well plates. Fresh blood was obtained from three healthy volunteers (donors 1, 2 and 3; all donors gave informed consent) and collected in Venosafe terumo citrated tubes (final citrate concentration 3.2 w/v%) (Terumo Europe N.V., Leuven, Belgium). Fresh platelet poor plasma (PPP) was obtained by a centrifugation step. The samples were submerged in 300  $\mu\text{L}$  of PPP and incubated for 30 min. After the incubation time, 80  $\mu\text{L}$  of the incubated PPP of all samples was put into round bottom 96 well plates and 20  $\mu\text{L}$  MP reagent was added to all wells. The plates were placed on a heater at 37 °C for 10 min subsequently. Then, 20  $\mu\text{L}$  of FluCa reagent was used to start the thrombin generation and the calibrated automated thrombogram (CAT) assay was carried out as published earlier [2].

The leukocyte adhesion test was performed using the blood of donors 4, 5 and 6 in 4 mL sodium heparin tubes (final concentration 68 IU) (Becton & Dickinson, Franklin Lakes, USA) and experiments

were done in triplicate. The samples of the leukocyte adhesion test were washed twice with sterile physiological saline solution and then incubated with 750  $\mu\text{L}$  of blood for one hour at room temperature under gentle shaking. The incubated blood was analysed using a Sysmex XE-5000 (Germany).

For the hemolysis test, fresh blood of three other donors (donors 7, 8 and 9; all donors gave informed consent) was collected in 4 mL sodium heparin tubes (final concentration 68 IU) (Becton & Dickinson, Franklin Lakes, USA) as well. Then, 600  $\mu\text{L}$  of blood was added to the membrane samples and controls, in duplo. The samples were incubated for one hour at room temperature under gentle shaking. Then, the incubated blood was centrifuged at 4000 rpm for 6 min and the supernatant was analysed using light absorbance at 542 nm. The percentage of hemolysis was calculated as follows:

$$\text{hemolysis percentage} = \frac{C_{\text{sample}} - C_{\text{neg}}}{C_{\text{pos}} - C_{\text{neg}}} * 100\% \quad (3)$$

where  $C_{\text{sample}}$  is the concentration of free hemoglobin in the sample ( $\mu\text{mol L}^{-1}$ ),  $C_{\text{neg}}$  is the free hemoglobin concentration in the negative saline control ( $\mu\text{mol L}^{-1}$ ) and  $C_{\text{pos}}$  is the concentration of free hemoglobin in the positive water control ( $\mu\text{mol L}^{-1}$ ).

For all tests, except for the lactate dehydrogenase assay (LDH), the complement tests and the hemolysis test, o-rings were used to keep the samples on the bottom of the well plates. The interaction of blood to the o-rings alone was taken into account as a control of the experiments. Furthermore, the PES-PVP membranes were used as a negative control for every blood compatibility test, except for the hemolysis test, where saline was used as a negative control. The positive controls varied and were adjusted to the type of blood compatibility tests. The glass coverslips were used as positive control for the qualitative platelet adhesion tests and thrombin generation tests. The PES-50 kDa membranes were used as controls for the quantitative platelet adhesion and leukocyte adhesion tests. Sterile ultrapure water was used as positive control for the hemolysis tests and RC58, DE81 and PES-50 kDa membranes were used for the complement activation experiments.

## 2.4. Statistics

Statistical analyses were performed using GraphPad PRISM version 5.00 software package. ANOVA and post-Tukey with significance level set to  $p < 0.05$  was used to determine statistical difference.

## 3. Results and discussion

### 3.1. Membrane characterization

Fig. 2 presents typical SEM images of the cross-sections of the flat-sheet membranes studied here. All membranes were mechanically stable and could be handled well in all characterisation tests.

The PES-PVP and PES membranes (Fig. 2A, E) both have an asymmetric pore morphology: a dense selective layer and finger-like pores on the air-side and a layer with macrovoids on the glass-side, as a result of the slower exchange between NMP and water, the solvent in the polymer solution and the non-solvent in the coagulation bath, respectively. The addition of 2 wt% SS to PES also results in membranes (PES-SS2 in Fig. 2B) with a dense selective layer and finger-like pores on the air-side, but with larger macrovoids on the glass-side. By increasing the amount of SS from 2 wt% to 4 and 6 wt%, the membranes' glass-sides present smaller and more finger-like macrovoids (Fig. 2B, C and D), similar to the pristine PES membrane of Fig. 2E. This is possibly due to the higher amount of polymer present in the PES-SS4 and PES-SS6 membranes. Fig. 2F presents the PES-50 kDa membrane with a selective layer and small finger-like pores on top of a support layer.

Fig. 3 shows typical ATR-FTIR spectra of the prepared flat-sheet membranes which were used to investigate the distribution of SS in the

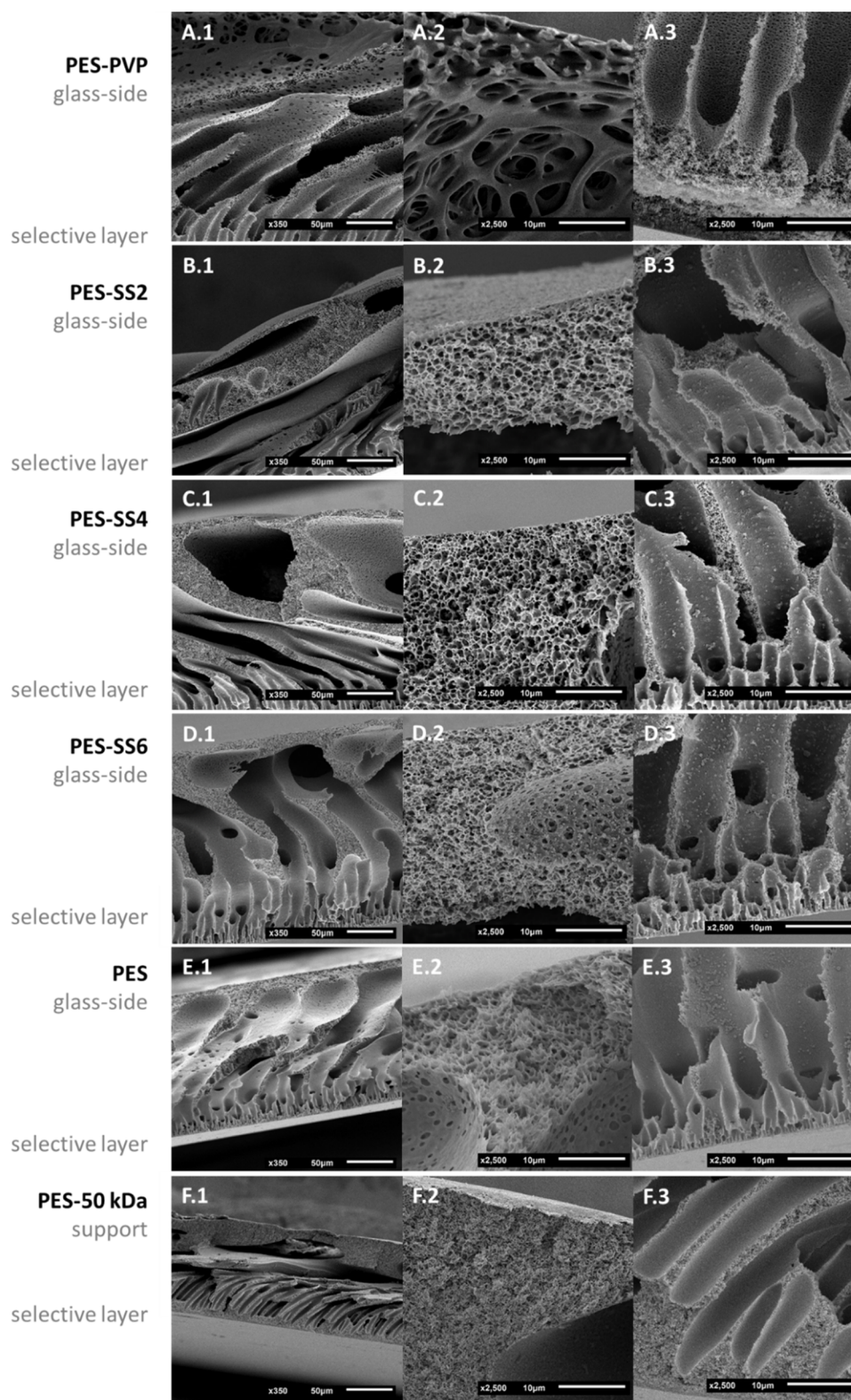


**Fig. 2.** Typical SEM images of the flat-sheet membranes: PES-PVP (A), PES-SS2 (B), PES-SS4 (C), PES-SS6 (D), PES (E) and PES-50 kDa (F). The magnifications are: images of column 1:350 $\times$ , size bar 50  $\mu\text{m}$  and images of columns 2 and 3:2500 $\times$ , size bar 10  $\mu\text{m}$ . Images of column 2 show the glass-side, whereas the images of column 3 show the air-side/selective layer.

PES-SS blend membranes. Just like the PES-PVP membranes, the SS membranes show a characteristic peak at 1680  $\text{cm}^{-1}$  corresponding to the carbonyl groups of NVP (the hydrophilic block of SS). Besides, the SS membranes show another characteristic peak at 1740  $\text{cm}^{-1}$  corresponding to the ester group of BMA (the hydrophobic block of SS) [32].

As expected, the spectrum of the pure PES membranes shows no peaks at these wavelengths, because PES has no carbonyl or ester groups (Fig. 3A). However, the peak at 1680  $\text{cm}^{-1}$  suggests the presence of a hydrophilic additive inside the commercial PES-50 kDa membranes. The characteristic SS peaks at 1680  $\text{cm}^{-1}$  and 1740  $\text{cm}^{-1}$  are observed

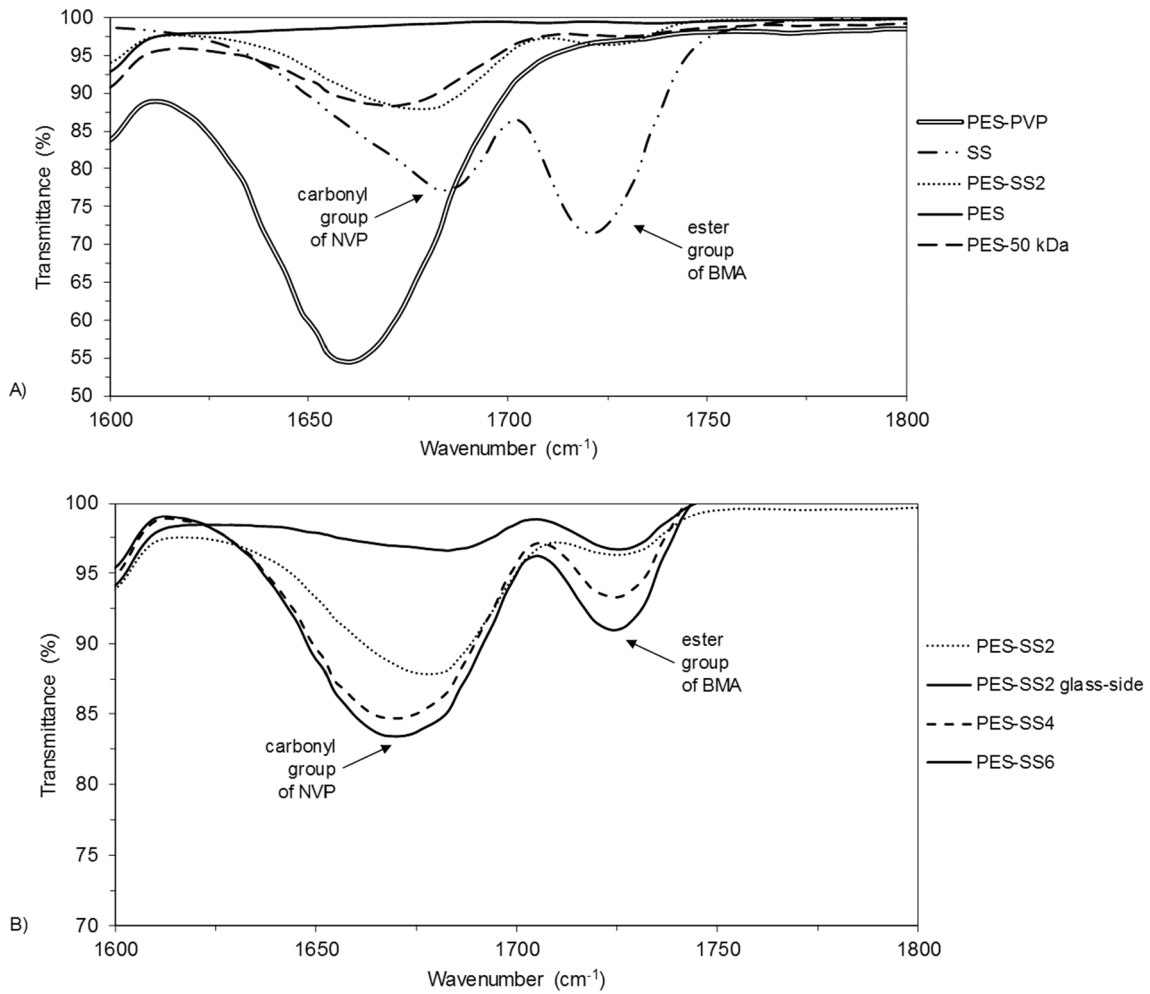


**Fig. 3.** (A) ATR-FTIR spectra of air-sides of PES-PVP, SS, PES-SS2, PES and PES-50 kDa membranes,  $n = 3$ . The characteristic peak at  $1680\text{ cm}^{-1}$  corresponds to the carbonyl groups of NVP (the hydrophilic part of the membrane that should ensure low protein adsorption and therefore higher membrane fouling resistance and blood compatibility). This characteristic peak is present for all membrane types (PES-PVP, SS, PES-SS2 and PES-50 kDa), except for the PES membrane. (B) ATR-FTIR spectra of PES-SS2 (both air-side and glass-side), PES-SS4 (air-side) and PES-SS6 membranes (air-side),  $n = 3$ . More SS is present on the air-sides than the glass-sides of the PES-SS blend membranes. Moreover, higher concentrations of SS are observed for PES-SS4 and PES-SS6 membranes than PES-SS2 membranes.

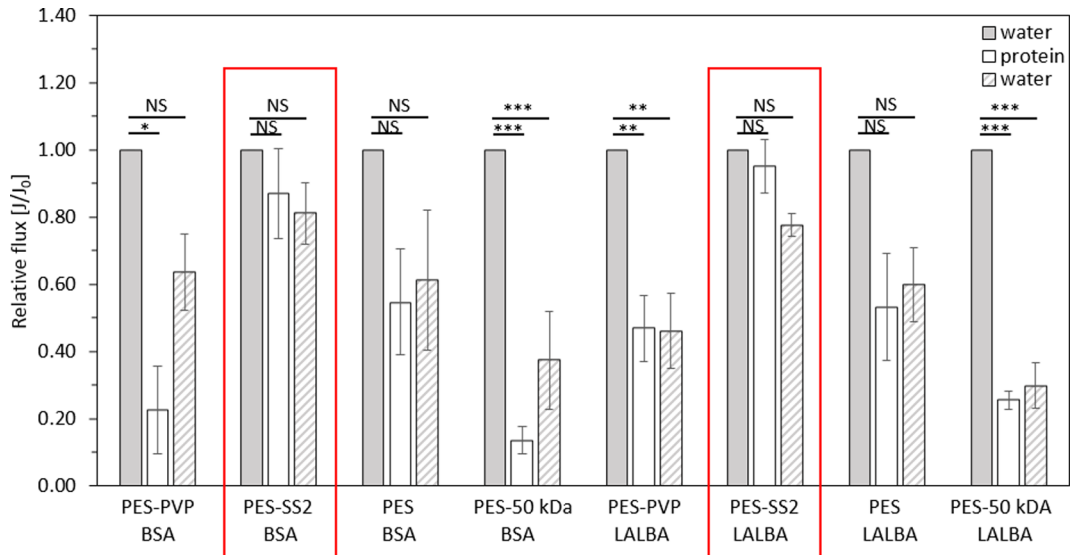


**Fig. 4.** Protein fouling experiments with flat-sheet membranes at 1 bar: PES-PVP, PES-SS2, PES and PES-50 kDa. The relative flux was determined first using water, then with BSA or LALBA in PBS solution, and finally using water again. The error bars show standard deviation ( $n = 3$ ).



**Table 2**  
Transport data of PES-PVP, PES-SS2, PES and PES-50 kDa membranes, measured at 1 bar ( $n = 3$ ).

Membrane	UF coefficient	$J_{\text{water}} (\text{mL} \cdot \text{h}^{-1} \cdot \text{m}^{-2} \cdot \text{mmHg}^{-1})$	$J_{\text{water}} (\text{L} \cdot \text{m}^{-2} \cdot \text{h}^{-1})$	$J_{\text{BSA}} (\text{L} \cdot \text{m}^{-2} \cdot \text{h}^{-1})$	$J_{\text{water}} (\text{L} \cdot \text{m}^{-2} \cdot \text{h}^{-1})$	FRR <sub>after BSA</sub> (%)	SC <sub>BSA</sub>	$J_{\text{water}} (\text{L} \cdot \text{m}^{-2} \cdot \text{h}^{-1})$	$J_{\text{LALBA}} (\text{L} \cdot \text{m}^{-2} \cdot \text{h}^{-1})$	$J_{\text{water}} (\text{L} \cdot \text{m}^{-2} \cdot \text{h}^{-1})$	FRR <sub>after LALBA</sub> (%)	SC <sub>LALBA</sub>
PES-PVP	461	346 ± 10	79 ± 46	220 ± 33	64	0.02 ± 0.01	419 ± 92	210 ± 20	197 ± 12	47	0.42 ± 0.01	
PES-SS2	75	56 ± 17	49 ± 16	46 ± 16	82	0.30 ± 0.11	38 ± 3	36 ± 5	29 ± 1	76	0.49 ± 0.27	
PES	295	221 ± 35	117 ± 17	131 ± 32	59	0.01 ± 0.02	367 ± 50	191 ± 32	217 ± 10	59	0.80 ± 0.23	
PES-50 kDa	981	736 ± 273	93 ± 7	249 ± 42	34	0.02 ± 0.01	634 ± 198	159 ± 33	182 ± 16	29	0.87 ± 0.21	

in the spectra of the PES-SS blend membranes, as well (Fig. 3A and B). The intensity of the peaks increases with an increase in SS concentration inside the membrane: the highest intensity is found in PES-SS6 membranes and lowest in PES-SS2 membranes (Fig. 3B). Importantly, the PES-SS2 spectra (Fig. 3B) show that there is a higher amount of carbonyl and ester groups on the air-side than on the glass-side of the membrane. This indicates that during membrane formation, SS polymer migrates towards the water non-solvent phase and, thus, resulting in membranes with higher SS concentration in the selective layer [33]. Similar phenomenon is also observed for PES-SS4 and PES-SS6 membranes where higher concentrations of SS are found at the selective layer of the membrane.

### 3.2. Membrane transport properties

During membrane preparation, we noticed that the polymer solutions of PES-SS4 and PES-SS6 were somewhat turbid indicating phase separation in solution, similar to the observations of Song et al. for blends with copolymer amounts higher than 5 wt% [33]. Based on this apparent immiscibility issue, the PES-SS2 membranes were selected for further studies concerning membrane fouling and were compared to the controls, PES-PVP, PES and PES-50 kDa membranes.

*Protein transport studies - membrane fouling studies:* Membrane fouling due to, for example, protein adsorption on the surface or pore blocking remains as one of the key factors that hampers membrane performance over time. Self-evidently, hemodialysis membranes work in direct contact with blood, so high membrane resistance to protein fouling can only benefit this application. In this section, we measured the transport of water, BSA and LALBA solutions through our membranes and we evaluated the fouling resistance by measuring the FRR of PES-PVP, PES-SS2, PES and PES-50 kDa membranes after permeation of BSA and LALBA solutions. Fig. 4 and Table 2 present the change of membrane flux due to protein transport as well as the change of water flux before and after the protein transport. Moreover, Table 2 presents the membranes' ultrafiltration (UF) coefficient.

For the PES-SS2 membranes, there is no significant difference between the permeance of BSA solution and LALBA solution and both clean water permeance values (the first and third bar of Fig. 4) indicating very low membrane - protein interaction. This happens even though both BSA and LALBA can penetrate into the membrane pores (sieving coefficient of BSA is 0.30 and of LALBA is 0.49, respectively). In contrast, the BSA solution permeance of the PES-PVP, PES and PES-50 kDa membranes is much lower than the clean water permeance. This can be due to either the impact a higher flux has on membrane fouling, or to the protein interaction with the membranes. Moreover, the significant difference between the first and third clean water permeance of PES-50 kDa membranes shows that these membranes without hydrophilic additive have poor flux recovery. The low membrane - protein interaction of the PES-SS2 membranes is also still evident when the smaller protein LALBA is used. In fact, the results of membrane selectivity (see sieving coefficients in Table 2) show that LALBA can penetrate into the pores of all membranes, though the flux recovery of the PES-SS2 membranes is the highest (PES-SS2, FRR ~ 80% whereas PES-PVP, PES and PES-50 kDa membranes have FRR ~ 50%, FRR ~ 60% and FRR ~ 30%, respectively). The improvement concerning fouling behaviour could be attributed to the presence of SS, especially its hydrophilic NVP block, on the selective layer and inside the pores of PES-SS2 membranes which prevents protein adsorption. For comparison, Susanto et al. developed PES-PVP and PES-PEG blend membranes with similar BSA SC to this study (SC = 0.29 and SC = 0.28 respectively), but they have much lower BSA FRR than our PES-SS2 membranes (approximately 28% and 15%, respectively) [9]. Furthermore, the PES-copolymer 3 wt% blend membranes reported by Song et al. have lower BSA SC (0.05) than our PES-SS2 membranes and have BSA FRR in the same range (81.97% for PES-copolymer 3 wt% blend membranes) [33]. This study has shown that the BSA SC can be decreased from 0.83

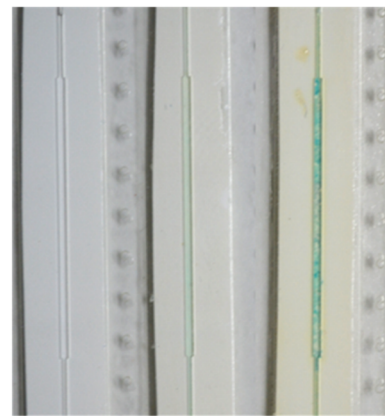
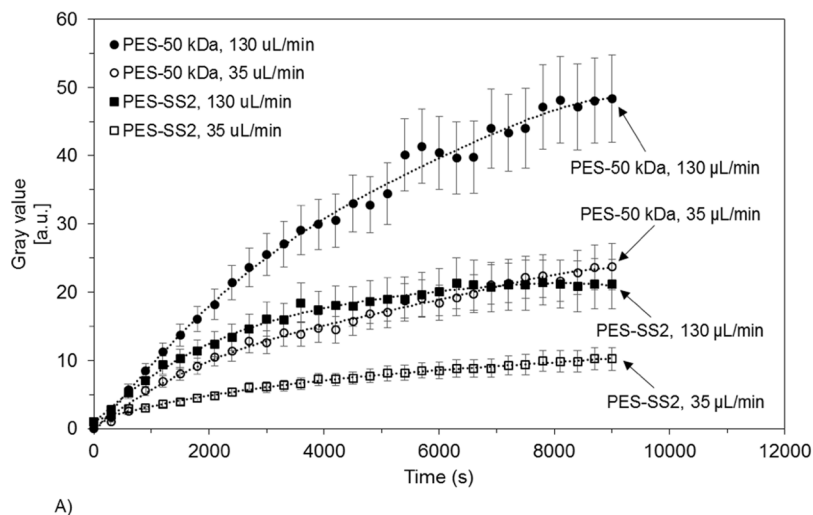


**Fig. 5.** Microchip LALBA fouling results ( $n = 3$ ). (A) LALBA fouling behaviour of PES-SS2 (squared data points) and PES-50 kDa (round data points) membranes at 35  $\mu\text{L}/\text{min}$  (open symbols) and 130  $\mu\text{L}/\text{min}$  (black symbols). (B) Macroscopic view of studied membranes in microchip: virgin PES-50 kDa membrane (left), fouled PES-SS2 membrane (centre) and fouled PES-50 kDa membrane (right).

(pristine SS membrane [2]) to 0.30 by blending SS and PES. Since hemodialysis membranes should have little or no albumin leakage, we plan to develop PES-SS2 hollow fiber membranes suitable for hemodialysis with even lower albumin SC in order to retain albumin in the future.

All the above results clearly show that the PES-SS2 membranes have higher fouling resistance in comparison to the control membranes. However, all these experiments were done using dead-end filtration at a 1 bar transmembrane pressure and for a certain time period. During dialysis, the proteins flow across the surface of the membrane. It is therefore important that one also evaluates the protein adhesion during flow of the solutions above the membrane surface. To achieve this, we used a microchip device and fluorescent-labelled LALBA under cross-flow conditions at  $\text{TMP} = 0$ . To mimic, as close as possible the dialysis process, we designed the chip channel dimensions and selected the flow rates of the applied protein solutions (35–130  $\mu\text{L}/\text{min}$ ) in order to obtain Reynolds numbers of 1.3–4.7, which are in the same range to the Reynolds numbers in a dialyzer membrane module (0.5–2, corresponding to blood flow rates 150–400  $\text{mL}/\text{min}$ ) [34]. Fig. 5 compares the results for the PES-50 kDa and PES-SS2 membranes. In Fig. 5A, the adhesion of the protein onto the membrane channel is presented in form of the grey scale values (high values indicate higher adhesion of the LALBA on the membrane surface), whereas in Fig. 5B, it is presented in form of dye staining (intense membrane coloration demonstrates a higher concentration of LALBA on membrane surface). The results of Fig. 5 clearly show that the PES-SS2 membrane has much lower interaction with the LALBA (corresponding to much lower grey scale and lower dye staining) in comparison to the commercial PES-50 kDa membrane, clearly indicating again the higher fouling resistance of the PES-SS membrane. For both membrane types, an increase in flow rate results in an increase in gray value (Fig. 5A). Possibly, the increase of the flow rate and the corresponding reduction of the thickness of the diffusive boundary layer leads to an increase of the adsorption rate. Besides, LALBA might suffer from higher shear stress at higher flow rates, resulting in unfolding of the protein and facilitated membrane – protein interactions [35]. Nevertheless, for both flow rates the performance of the PES-SS is superior to the performance of the PES-50 kDa membrane.

### 3.3. Blood compatibility studies

Besides the high fouling resistance, an excellent membrane blood compatibility is a crucial prerequisite for application in dialysis therapy. Therefore, we performed here an extensive study of the blood compatibility of the developed PES-SS2 membranes and we compared it to benchmark membranes. Fig. 6(A) presents typical SEM images of pristine surfaces (Fig. 6(A, column 1)) and adhered platelets on the materials' surfaces (Fig. 6(A, columns 2–4)). In addition to platelet adhesion, both platelet aggregation and activation were investigated too. When platelets adhere onto dialyzer membranes, they can form for instance aggregates that block the blood flow or cause neutrophils to generate reactive oxygen species [2]. The PES-SS2 membranes show little platelet adhesion, aggregation and activation. Besides, the platelets that do adhere to the surface are flat and roundly shaped without pseudopodia (Fig. 6B2-4). In contrast, the PES-50 kDa membranes (Fig. 6C2-4) demonstrate higher platelet adhesion with platelets having both a more spherical shape and small pseudopodia. Moreover, deposits of both single adhered platelets as well as clusters of platelets with long pseudopodia and spherical shapes are observed on the surfaces of PES-PVP membranes (Fig. 6A2-4) and glass (Fig. 6D2-4), indicating activation of the adhered platelets. Apparently, the optimal distribution of hydrophobic and hydrophilic patches in PES-SS2 membranes, prevents protein adhesion onto the surface and for this reason platelet adhesion and activation is averted as well. The quantitative test results of Fig. 6(B,C) show similar trend in platelet adhesion for all membranes, though one could argue that the LDH assay results show that platelets adhere less onto PES-PVP membranes. However, the SEM images (Fig. 6A3-4 and B3-4) show that the adhered platelets of the PES-PVP membrane in contrast to the adhered platelets of the PES-SS2 membrane, have changed into their activated state. This means that in time, the adhered platelets of the PES-PVP membrane would release the contents of their granules, resulting in the activation and eventually adhesion of more platelets and other cells as well [36,37].

In addition to platelet adhesion, any activation of the patients' complement system because of blood-membrane contact is an important indicator of blood compatibility as well. Therefore, the average percentage of the classical and alternative pathway complement

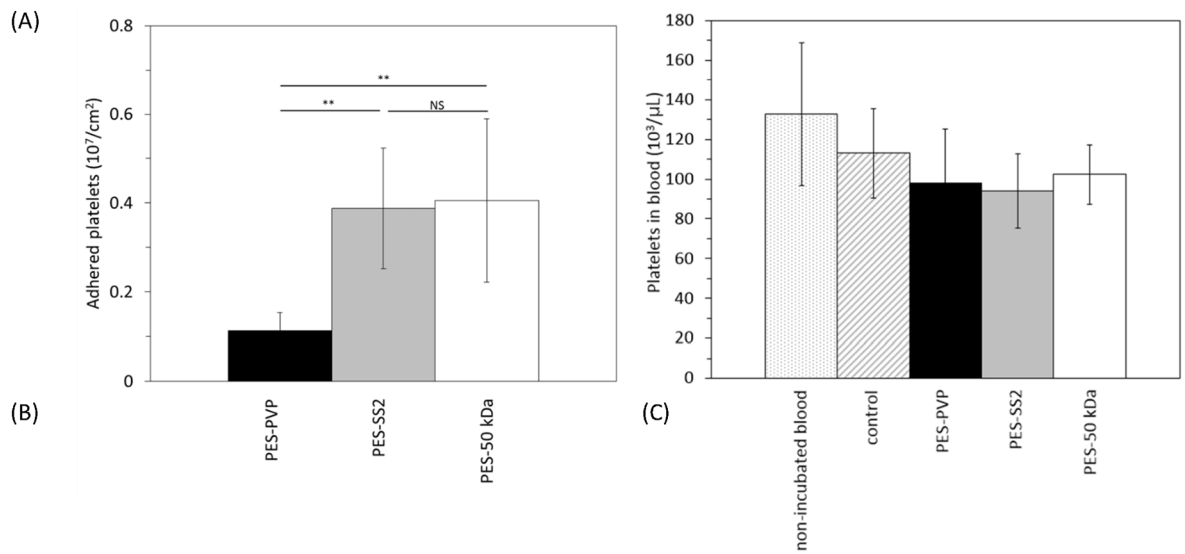
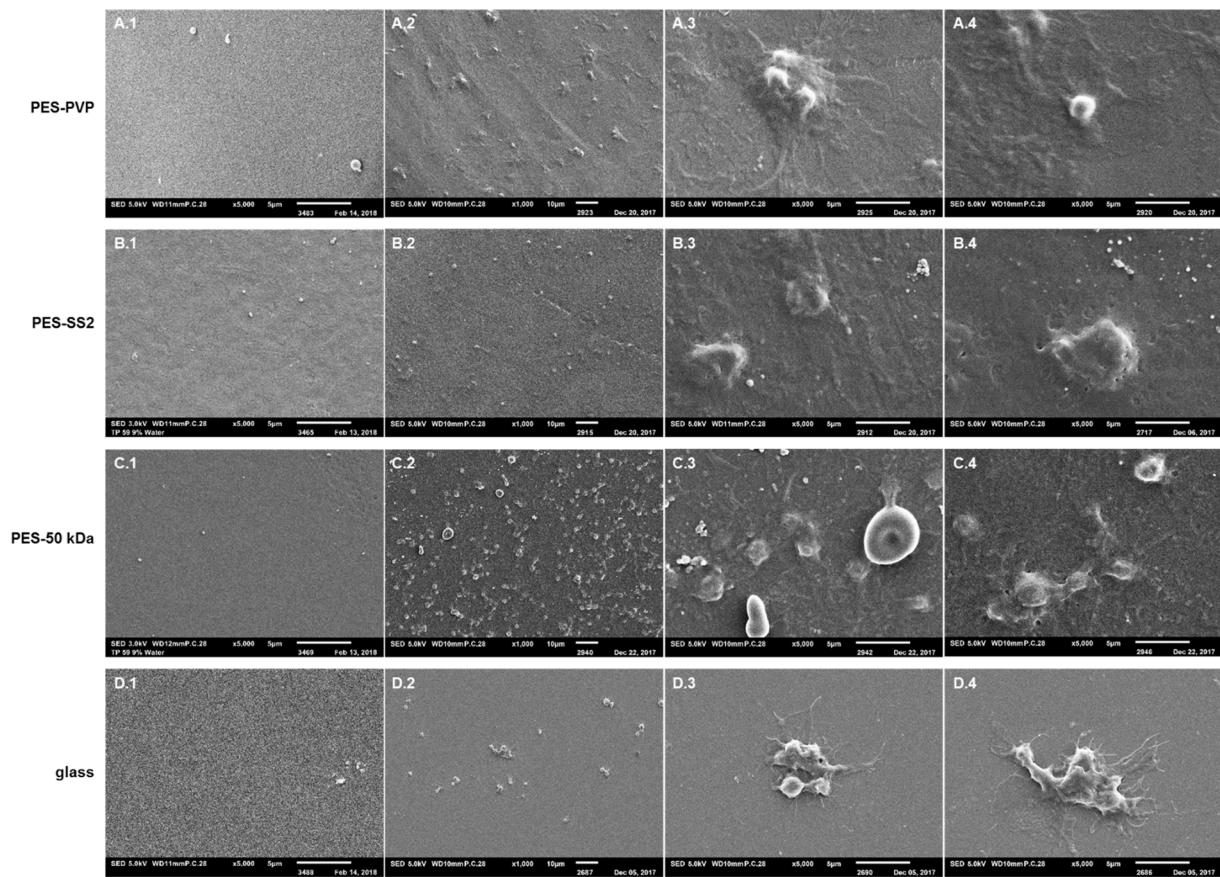


**Fig. 6.** (A) Typical SEM pictures of adhered platelets on PES-PVP (A2-4), PES-SS2 (B2-4), PES-50 kDa (C2-4) membranes and glass (D2-4). Images A.1, B.1, C.1 and D.1 show pristine materials. Surface images with magnifications of  $5000\times$  (1,3 and 4) and  $1000\times$  (2). (B) Average number of adhered platelets per  $cm^2$  of material presented for the following membranes: PES-PVP, PES-SS2 and PES-50 kDa. Error bars indicate standard deviation ( $n = 2$ , for donors 4, 5 and 6). (C) Average number of platelets present in blood. For non-incubated blood, control (incubated blood), PES-PVP, PES-SS2 and PES-50 kDa membranes. Error bars indicate standard deviation ( $n = 3$ , for donors 4, 5 and 6).

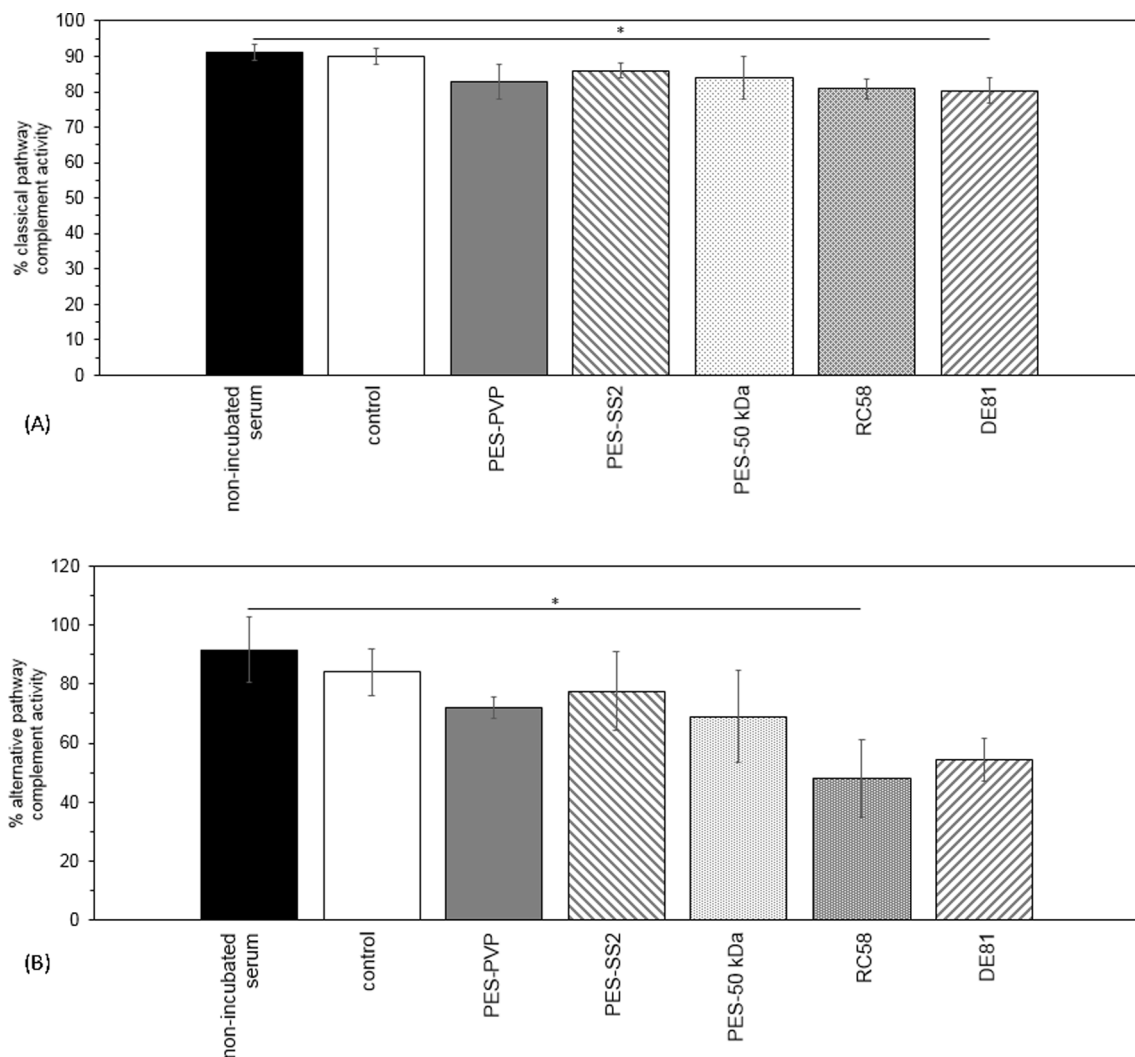


**Fig. 7.** Average percentage classical pathway (A) and alternative pathway (B) complement activity in serum of donors 1, 2 and 3. For non-incubated serum, control (incubated serum), PES-PVP, PES-SS2, PES-50 kDa, RC58 regenerated cellulose and DE81 DEAE cellulose membranes. No significant differences in both classical and alternative pathway complement activity are observed for the different types of membranes, except for the cellulose-based membranes. Error bars indicate standard deviation ( $n = 2$ ).

activation is shown in Fig. 7. For both pathways, there is no significant difference between the complement activity of the non-incubated serum samples and the control samples (incubated serum samples), see first two bars in Fig. 7. Therefore, any observed decrease in activity originates from the membrane activating the complement system via either the classical pathway, the alternative pathway or both. None of the investigated membranes is likely to activate the complement system via the classical or alternative pathway, except the DE81 and RC58 membranes of Fig. 7A and B respectively. These cellulose membranes show a significant decrease in complement activity.

Furthermore, a thrombin generation test is used to evaluate whether or not the membrane materials trigger the coagulation of patients' blood. If they do, the enzyme thrombin is generated and it converts, among other things fibrinogen into fibrin, the primary ingredient of a clot [38]. A prothrombotic state is defined by (1) a short lag time, which is the initiation phase of thrombin generation and is the time that is necessary for the generated thrombin to reach 1/6 of the peak concentration, and (2) a high thrombin peak height, which is the rapid thrombin concentration increase in the propagation phase of thrombin generation [38]. Fig. 1A and B of Appendix B show a significant difference between both the lag time and peak height of the glass samples (positive control) and the incubated PPP controls (negative control). The lag time of our PES-SS2 membranes is between the negative and

positive control. Moreover, the thrombin peak height of the PES-SS2 membranes is significantly lower than the peak height of the positive glass control, indicating that the PES-SS membranes do not activate the intrinsic coagulation pathway.

The PES-SS2 membranes performed very well in the haematology tests too. The average number of leukocytes that are present in the blood after incubation with PES-PVP, PES-SS2 and PES-50 kDa membranes is comparable for all membranes (see Appendix B, Fig. 2). Furthermore, the number of leukocytes present in every donors' blood is in the normal range (see Appendix B, first bar in Fig. 2). Moreover, the number of leukocytes in the non-incubated blood samples and their controls, the incubated blood samples, are in similar range. This means that the well plates and rubber rings have no influence on the adhesion of the leukocytes. Finally, the results of the hemolysis test are presented in the Table B.1. All tested membranes have an average hemolysis percentage lower than 5% and therefore considered as non-toxic, according to the ASTM F-756-08 standard [2]. The PES-SS2 membranes have comparable good results for the hemolysis percentage as the benchmark PES-PVP membranes.

Overall, all the above studies show that the PES-SS2 membranes have very good blood compatibility performance and therefore are suitable for application in dialysis therapy.

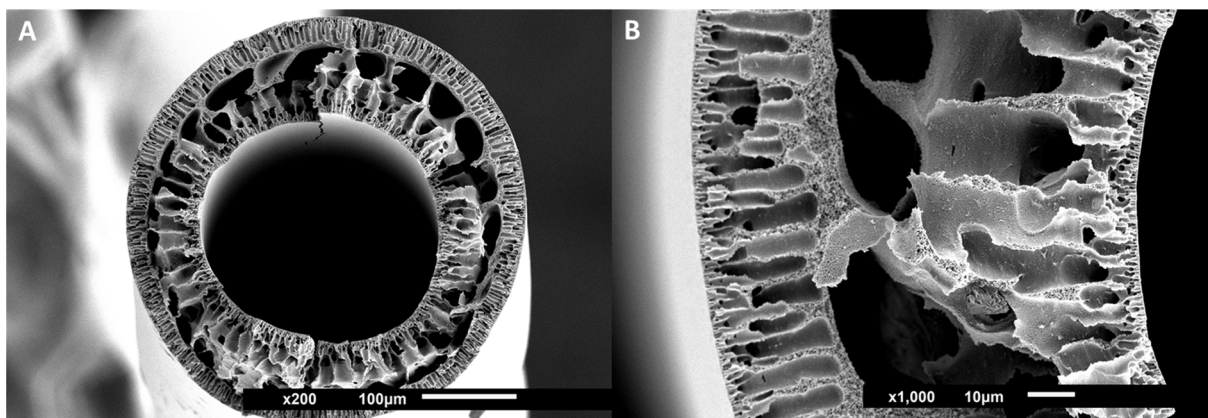


**Fig. 8.** SEM images of hollow fiber PES-SS2 membranes. Images show cross-sections with magnifications of 200 $\times$ , size bar 100  $\mu\text{m}$  (A) and 1000 $\times$ , size bar 10  $\mu\text{m}$  (B), zoom-in.

#### 4. Conclusions and outlook

This study presents for the first time the successful development of low fouling, blood compatible membranes based on blends of PES and SlipSkin™. Our results show that the membranes with SS of 2 wt% (PES-SS2) have increased hydrophilicity, higher fouling resistance to proteins and middle-size molecules (better than benchmark membranes) and very good blood compatibility, comparable to benchmark membranes.

Based on the protocol for fabrication of flat-sheet PES-SS2 membranes (see earlier) we actually also performed preliminary studies for fabricating PES-SS2 hollow fiber membranes, see Fig. 8 (details about their fabrication is given in the Appendix C).

These first PES-SS2 fibers have dense inner and outer layers and in between finger-like pores and larger macrovoids. Despite that, their mechanical properties are quite good and the membranes can be

handled easily. Their clean water permeance is  $7 \pm 3 \text{ L m}^{-2} \text{ h}^{-1} \text{ bar}^{-1}$  (measured at the TMP-range of 1–2 bar) and it is lower than that of the PES-SS2 flat-sheet membranes ( $56 \pm 17 \text{ L m}^{-2} \text{ h}^{-1} \text{ bar}^{-1}$ ). Future studies will focus on further optimization of these fibers and to the detailed investigation of their performance for filtration of uremic toxins from human plasma and full blood.

#### Funding

This work was supported by Health~Holland KidneyPort [project number 40-43100-98-009]; and EU Marie Curie ITN BIOART [project number 316690].

#### Declaration of Competing Interest

None.

#### Appendix A. Microfluidic chip fouling experiments

##### A.1. Labelling of LALBA

In order to monitor the LALBA distribution and adhesion over time at zero TMP with the microchip, the proteins need to be labelled first following the protocol of Greene et al. [31]. In short, LALBA was dissolved in sodium bicarbonate buffer to obtain a concentration of 10 mg/mL. Subsequently, reactive dye was dissolved in 20  $\mu\text{L}$  of DMSO of the labelling kit. After dissolution of both protein and corresponding dye, two mixtures were transferred into the same vial and stirred gently for 2 h. As the finishing step in the procedure, protein-dye conjugates were separated from free excess dye by gel filtration columns (size exclusion limit 5 kDa). To start the elution 5 mL of PBS was added. Solvent flow in the column was achieved by gravity only, without addition of extra pressure. The final protein concentration (mg/mL) was calculated as follows:

$$c_{\text{protein}} = \frac{A_{280} - 0.05 \cdot A_{647}}{\epsilon_{\text{protein}}} \cdot MW_{\text{protein}} \cdot \text{dilution factor} \quad (\text{A.1})$$

where  $A_{647}$  is absorbance of the conjugate at 647 nm,  $A_{280}$  is the absorbance of the conjugate at 280 nm,  $\epsilon_{\text{protein}}$  is the molar extinction coefficient of protein ( $27,400 \text{ cm}^{-1} \text{ M}^{-1}$ ) at 280 nm,  $MW_{\text{protein}}$  is the molecular weight of the protein (g/mol) and the dilution factor is the dilution of the labelled conjugate prior to the absorbance measurement. A dilution factor of 10 was used in order to obtain a maximum absorbance in the range from 0.5 to 1. The absorbance of the conjugates was measured with a Libra S12 UV-spectrophotometer (Biochrom, UK). The final conjugate solution was diluted with PBS in order to achieve a concentration of 50 mg/L as it corresponds to clinically relevant median concentrations of  $\beta_2$ -microglobulin in human blood [35].

##### A.2. Experimental set-up

The filtration experiments were performed with two systems: (1) a Zeiss Axio Observer.zlm inverted microscope equipped with a HXP 120C power supply (Zeiss Axio Vision Software), a filter set 38 (to detect the fluorescence of  $\alpha$ -lactalbumin-Atto-647 N), and an automated stage and (2) a Fluigent MFCS-Flex pressure controller, combined with a FLOWELL flow-controller (MAESFLO software). A total of 3 pressure and 3 flow controllers were used. Two pressure controllers can supply a pressure of up to 1000 mbar, while the other one goes up to 350 mbar. As for the flow controllers, the first one can operate at a maximum flow of 7715  $\mu\text{L}/\text{min}$ , the second one at maximum flow of 55  $\mu\text{L}/\text{min}$ , and the last one at a maximum flow of 1100  $\mu\text{L}/\text{min}$ . The microfluidic chips were connected to the tubes of the pressure-flow controller and placed on the microscope stage to start the experimental protocol (Fig. A1).

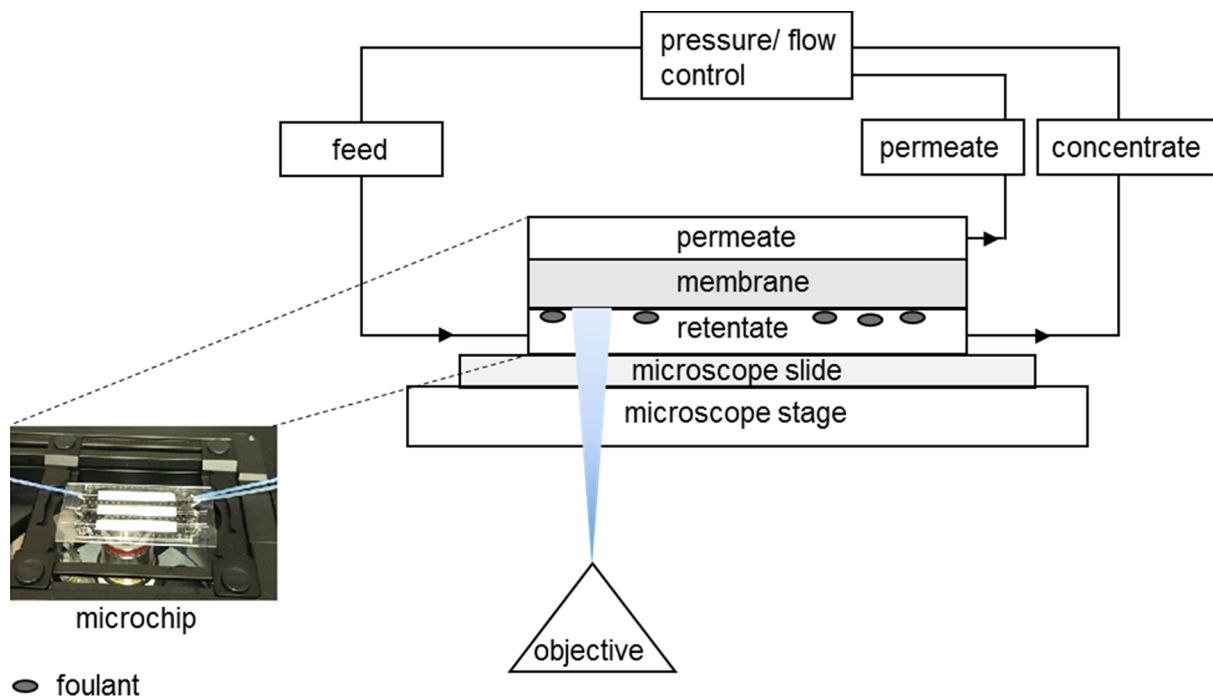


Fig. A1. Schematic representation of the experimental set-up used combining the fluorescent microscope and the microchip.

## Appendix B. Biocompatibility tests

### B.1. Coagulation - thrombin generation

Here, the intrinsic coagulation pathway is studied, because thrombin formation is triggered with phospholipids and calcium ions in this test, rather than with tissue factor [2]. Fig. B1A and B show the thrombin lag time and peak height of the different samples, respectively.

### B.2. Hematology - leukocyte adhesion and hemolysis

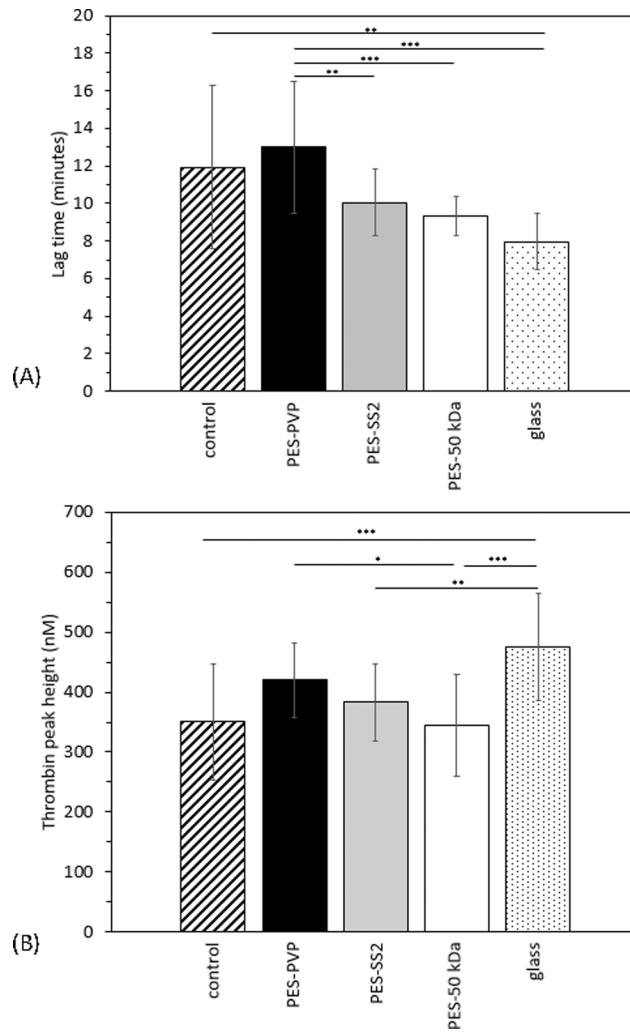
Fig. B2 shows the average number of leukocytes (as percentage of initial value) that are present in the blood after incubation with PES-PVP, PES-SS2 and PES-50 kDa membranes. In general, the adhesion of leukocytes to the PES-SS2 membranes is comparable to the PES-PVP membranes.

Table B.1 presents the average hemolysis percentage of the membranes and controls. The well-plate has little effect on the average hemolysis percentage, as shown by the non-incubated and incubated blood samples (Table B.1). More importantly, the average hemolysis percentage of all membranes is lower than 5%, indicating their non-toxicity [2].

**Table B1**

Average percentage hemolysis (%)  $\pm$  standard deviation ( $n = 2$  of donors 7, 8 and 9).

Membrane	Hemolysis (%)
Non-incubated sample	0.01 $\pm$ 0.01
Control (incubated blood)	0.09 $\pm$ 0.03
PES-PVP	1.01 $\pm$ 0.17
PES-SS2	0.96 $\pm$ 0.17
PES-50 kDa	0.6 $\pm$ 0.05



**Fig. B1.** (A) Lag time in minutes and (B) peak height in nM of thrombin generation for control (incubated platelet poor plasma), PES-PVP, PES-SS2, PES-50 kDa membranes and glass ( $n = 3$ ).

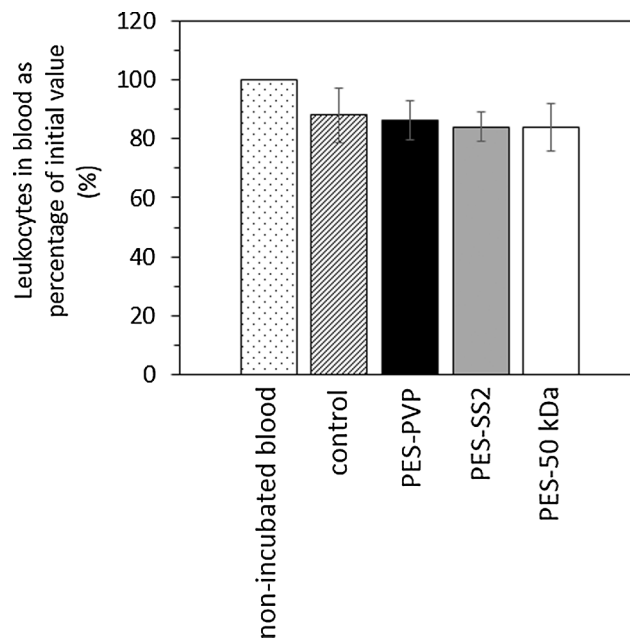


**Fig. B2.** Average number of leukocytes present in blood as percentage of initial value (%). For non-incubated blood, control (incubated blood), PES-PVP, PES-SS2 and PES-50 kDa membranes for donors 4, 5 and 6. Error bars indicate standard deviation ( $n = 3$ ).

## Appendix C. Fabrication of PES-SS2 hollow fibers

PES-SS2 hollow fiber membranes were prepared by dry-wet spinning via immersion precipitation. First, 15 wt% PES was dissolved in NMP and then 2 wt% SS was added. The polymer solution was mixed on a rollerbank for at least 48 h and degassed for 24 h before the spinning process.

The polymer solutions were pumped through the spinneret using a speed of 1 mL/min at room temperature (the dimensions of the spinneret are listed in Table C1 below). To create the bore, ultrapure water was pumped through the spinneret with a speed of 5.8 mL/min. After an airgap of 10 cm between the spinneret and the ultrapure water - coagulation bath, the fiber was collected using a pulling wheel with a speed of 18.6 m/min.

**Table C1**  
Fabrication conditions of the PES-SS2 hollow fiber membranes.

Spinning parameters	PES-SS2
Inner diameter needle of spinneret	0.2 mm
Outer diameter needle of spinneret	-
Inner diameter first orifice of spinneret	0.5 mm
Outer diameter first orifice of spinneret	0.8 mm
Inner diameter second orifice of spinneret	1 mm
Polymer dope pumping speed	1.0 mL/min
Bore liquid pumping speed	5.8 mL/min
Air gap	10 cm
Pulling wheel speed	18.6 m/min

## Appendix D. Supplementary material

Supplementary data to this article can be found online at <https://doi.org/10.1016/j.seppur.2019.05.049>.

## References

- [1] M.S.L. Tijink, et al., Mixed matrix hollow fiber membranes for removal of protein-bound toxins from human plasma, *Biomaterials* 34 (32) (2013) 7819–7828.
- [2] M. Tijink, et al., Development of novel membranes for blood purification therapies based on copolymers of N-vinylpyrrolidone and n-butylmethacrylate, *J. Mater. Chem. B* 1 (44) (2013) 6066–6077.
- [3] R. Vanholder, et al., Review on uremic toxins: classification, concentration, and interindividual variability, *Kidney Int.* 63 (5) (2003) 1934–1943.
- [4] A. Davenport, Portable and wearable dialysis devices for the treatment of patients with end-stage kidney failure: Wishful thinking or just over the horizon? *Pediat. Nephrol.* 30 (12) (2014) 2053–2060.
- [5] A. Davenport, et al., A wearable haemodialysis device for patients with end-stage renal failure: a pilot study, *Lancet* 370 (9604) (2007) 2005–2010.
- [6] W.H. Fissell, S. Roy, A. Davenport, Achieving more frequent and longer dialysis for the majority: wearable dialysis and implantable artificial kidney devices, *Kidney Int.* 84 (2) (2013) 256–264.
- [7] S. Eloot, I. Ledebro, R.A. Ward, Extracorporeal removal of uremic toxins: can we still do better? *Semin. Nephrol.* 34 (2) (2014) 209–227.
- [8] V. Gura, et al., Continuous renal replacement therapy for end-stage renal disease - The wearable artificial kidney (WAK), *Cardiovasc. Disorders Hemodial.* 149 (2005) 325–333.
- [9] H. Susanto, M. Ulbricht, Characteristics, performance and stability of polyethersulfone ultrafiltration membranes prepared by phase separation method using different macromolecular additives, *J. Membr. Sci.* 327 (1–2) (2009) 125–135.
- [10] M. Teodorescu, M. Bercea, Poly(vinylpyrrolidone) - a versatile polymer for biomedical and beyond medical applications, *Polym.-Plast. Technol. Eng.* 54 (9) (2015) 923–943.
- [11] S.Q. Nie, et al., Improved blood compatibility of polyethersulfone membrane with a hydrophilic and anionic surface, *Colloids Surfaces B-Biointerfaces* 100 (2012) 116–125.
- [12] Y.L. Su, et al., Modification of polyethersulfone ultrafiltration membranes with phosphorylcholine copolymer can remarkably improve the antifouling and permeation properties, *J. Membr. Sci.* 322 (1) (2008) 171–177.
- [13] Y. Koga, et al., Biocompatibility of polysulfone hemodialysis membranes and its mechanisms: involvement of fibrinogen and its integrin receptors in activation of platelets and neutrophils, *Artif. Organs* 42 (9) (2018) E246–E258.
- [14] M. Matsuda, et al., Effects of fluid flow on elution of hydrophilic modifier from dialysis membrane surfaces, *J. Artif. Organs* 11 (3) (2008) 148–155.
- [15] K. Namekawa, et al., Poly(N-vinyl-2-pyrrolidone) elution from polysulfone dialysis membranes by varying solvent and wall shear stress, *J. Artif. Organs* 15 (2) (2012) 185–192.
- [16] B. Madsen, et al., Effect of sterilization techniques on the physicochemical properties of polysulfone hollow fibers, *J. Appl. Polym. Sci.* 119 (6) (2011) 3429–3436.
- [17] W. Albrecht, et al., Modification of poly(ether imide) membranes with brominated polyvinylpyrrolidone, *J. Membr. Sci.* 291 (1–2) (2007) 10–18.
- [18] M. Miyata, et al., Influence of sterilization and storage period on elution of polyvinylpyrrolidone from wet-type polysulfone membrane dialyzers, *Asaio J.* 61 (4) (2015) 468–473.
- [19] K. Namekawa, et al., Longer storage of dialyzers increases elution of poly(N-vinyl-2-pyrrolidone) from polysulfone-group dialysis membranes, *J. Artif. Organs* 14 (1) (2011) 52–57.
- [20] X.L. Liu, et al., Poly(N-vinylpyrrolidone)-modified surfaces for biomedical applications, *Macromol. Biosci.* 13 (2) (2013) 147–154.
- [21] S. Konishi, et al., Eluted substances from hemodialysis membranes elicit positive skin prick tests in bioincompatible patients, *Artif. Organs* 39 (4) (2015) 343–351.
- [22] N. Nady, et al., Modification methods for poly(arylsulfone) membranes: A mini-review focusing on surface modification, *Desalination* 275 (1–3) (2011) 1–9.
- [23] C. He, et al., Graphene oxide and sulfonated polyanion co-doped hydrogel films for dual-layered membranes with superior hemocompatibility and antibacterial activity, *Biomater. Sci.* 4 (10) (2016) 1431–1440.
- [24] C.X. Nie, et al., Novel heparin-mimicking polymer brush grafted carbon nanotube/PES composite membranes for safe and efficient blood purification, *J. Membr. Sci.* 475 (2015) 455–468.
- [25] H.H.L. Hanssen, et al., Metallic wires with an adherent lubricious and blood-compatible polymeric coating and their use in the manufacture of novel slippery-when-wet guidewires: Possible applications related to controlled local drug delivery, *J. Biomed. Mater. Res.* 48 (6) (1999) 820–828.
- [26] C.C.L. Peerlings, et al., Heparin release from slippery-when-wet guide wires for intravascular use, *J. Biomed. Mater. Res.* 63 (6) (2002) 692–698.
- [27] R.T. Pijls, et al., Flexible coils with a drug-releasing hydrophilic coating: A new platform for controlled delivery of drugs to the eye? *Bio-Med. Mater. Eng.* 14 (4) (2004) 383–393.
- [28] Y.A. Liu, et al., Improved antifouling properties of polyethersulfone membrane by blending the amphiphilic surface modifier with crosslinked hydrophobic segments, *J. Membr. Sci.* 486 (2015) 195–206.
- [29] D. Pavlenko, et al., New low-flux mixed matrix membranes that offer superior removal of protein-bound toxins from human plasma, *Sci. Rep.* 6 (2016) 34429.
- [30] ISO, ISO 10993-4:2002/Amd 1:2006 - ICS : 11.100.20 Biological evaluation of medical devices, 2006(1).
- [31] L.H. Greene, et al., Stability, activity and flexibility in alpha-lactalbumin, *Protein Eng.* 12 (7) (1999) 581–587.
- [32] S.V. Kumar, et al., N-vinylpyrrolidone and ethoxyethyl methacrylate copolymer: Synthesis, characterization and reactivity ratios, *J. Macromol. Sci. Part A-Pure Appl. Chem.* 44 (10–12) (2007) 1161–1169.
- [33] H.M. Song, et al., Hemocompatibility and ultrafiltration performance of surface-functionalized polyethersulfone membrane by blending comb-like amphiphilic block copolymer, *J. Membr. Sci.* 471 (2014) 319–327.
- [34] S. Eloot, Experimental and Numerical Modeling of Dialysis, PhD dissertation Ghent University, 2004.
- [35] M. Meireles, P. Aimar, V. Sanchez, Albumin denaturation during ultrafiltration - effects of operating-conditions and consequences on membrane fouling, *Biotechnol. Bioeng.* 38 (5) (1991) 528–534.
- [36] S.H. Yun, et al., Platelet activation: the mechanisms and potential biomarkers, *Biomed. Res. Int.* (2016).
- [37] E.L.G. Prydzial, et al., Blood coagulation dissected, *Transfus. Apheres. Sci.* 57 (4) (2018) 449–457.
- [38] E. Castoldi, J. Rosing, Thrombin generation tests, *Thromb. Res.* 127 (2011) S21–S25.